A comparative study of optimized and unoptimized finite-difference and Runge–Kutta schemes in a 2D CAA benchmark

You Wei Ho* and Edward J. Brambley†
University of Warwick, Coventry CV4 7AL, United Kingdom

Dispersion Relation Preserving (DRP) optimized derivatives are widely used in computational aeroacoustics for efficiently representing waves with fewer points per wavelength. However, recent studies reveal that these derivatives may not perform as effectively for non-constant-amplitude waves, arising due to the underlying optimization process assuming a real wavenumber. Similarly, this limitation also potentially impacts optimized Runge–Kutta schemes, such as the Low Dispersion and Dissipation Runge–Kutta (LDDRK) schemes. In this paper, we explore these theoretical insights through a practical example of 2-D wave propagation within a canonical computational aeroacoustics (CAA) benchmark test case.

I. Introduction

The propagation of waves poses significant challenges across various scientific and engineering fields, including acoustics, electromagnetics, and seismology. In particular, computational aeroacoustics (CAA) has garnered extensive focus due to escalating environmental concerns and stringent noise emission standards. Despite the advancements, simulating aeroacoustic phenomena that involve wave propagation remains a formidable task. This complexity stems from the demanding computational requirements needed to accurately represent unsteady flow oscillations and the dispersive and dissipative characteristics of small-amplitude acoustic waves across entire computational domains, all while simultaneously ensuring numerical stability. In contrast to the typical amplitude scales addressed in Direct Numerical Simulation (DNS) and Large Eddy Simulation (LES), acoustic wave amplitudes encountered in CAA often approximate the level of numerical noise, as noted by [1]. Consequently, there is an imperative need for developing advanced numerical methodologies that enable precise, high-resolution CAA simulations at reduced computational costs with better numerical stability.

Recently, significant advancements in CAA simulations have primarily focused on optimizing spatial and temporal schemes for accurate calculation of wave propagation with few points per wavelength and time steps per wave period. Notably, key developments of optimized spatial derivatives include: the by-now classic 7-point 4th order explicit DRP schemes [2, 3]; optimized implicit/compact schemes of up to 6th order [4, 5]; prefactored implicit MacCormack schemes [6]; trigonometrically optimized schemes [7]; 2nd and 4th order 9, 11, and 13 point schemes [8]; and asymmetric optimized schemes for use near boundaries [9, 10]. For time-stepping, optimized timestepping schemes include: an optimized Adams–Bashforth scheme [2]; Low Dispersion and Dissipation Runge–Kutta (LDDRK) 5-step, 6-step and alternating 4/6- and 5/6-step schemes [11]; and optimized 5- and 6-step Runge–Kutta schemes [8]. Rona et al. [12] furthered this by attempting to jointly optimize spatial and temporal schemes for enhanced wave propagation, although this analysis is dependent on the dispersion relation of the system being simulated, while the previously mentioned schemes are applicable to general dispersion relations.

In this paper, we consider symmetric finite difference schemes on equally space grids $x_j = j\Delta x$. The theory below remains valid for implicit (i.e. compact) schemes, while a preliminary study for non-symmetric schemes is given in [13]. Given a function $f(x)$ evaluated at discrete points $f_j = f(x_j)$, the derivative $f'(x_j)$ is approximated by a $2N+1$ point scheme that can be represented by finite difference in the general form

$$a_0 f_i' + \sum_{m=1}^{M} a_m \left(f_{i+m}' + f_{i-m}'\right) = \frac{1}{\Delta x}\sum_{n=1}^{N} d_n \left(f_{i+n} - f_{i-n}\right). \tag{1}$$

*Research Fellow, Warwick Mathematics Institute, you.ho@warwick.ac.uk.
†Reader (Associate Professor), Warwick Mathematics Institute and WMG, E.J.Brambley@warwick.ac.uk, AIAA Senior Member.

Here, it is called an explicit scheme if $a_0 = 1$ and $M = 0$; otherwise, it is called an implicit scheme. We will restrict attention to explicit schemes in the rest of this paper. Traditionally, the choice of d_n is to give as accurate as possible a derivative for sufficiently small Δx. This choice would give $f_j' = f'(x_j) + O\big(\Delta x^{2N}\big)$, and such $2N$th order schemes are referred to here as maximal-order (MO) schemes. Alternatively, the coefficients d_n may be chosen to only require that $f_j' = f'(x_j) + O\big(\Delta x^{2L}\big)$ and to use the remaining $(N - L)$ degrees of freedom to optimize the resolution performance of the derivative. Substituting a wave with $f(x) = \mathrm{Re}\big(A\mathrm{e}^{\mathrm{i}\alpha x}\big)$ into (1) leads to the numerical dispersion

$$f_j' = \mathrm{Re}(\mathrm{i}\bar{\alpha}A\mathrm{e}^{\mathrm{i}\alpha x_j}), \qquad \text{where} \qquad \bar{\alpha}\Delta x = 2\sum_{n=1}^{N} d_n \sin(n\alpha\Delta x). \tag{2}$$

Hence, we aim for $\bar{\alpha}$ to closely approximate α in wave problems. Tam & Webb[2] chose $N = 3$ and $L = 2$, resulting in a 7-point derivative with fourth-order accuracy. They utilized the additional degree of freedom to minimize the error norm, given by

$$E = \int_0^{\eta} \left|\bar{\alpha}(\alpha)\Delta x - \alpha\Delta x\right|^2 \mathrm{d}(\alpha\Delta x), \tag{3}$$

with $\eta = \pi/2$. Tam & Shen[3] later recommended $\eta = 1.1$ for a more balanced approach, and this adjustment has been widely adopted in modern schemes. These optimized methods are known as Dispersion Relation Preserving (DRP) schemes. Traditionally, these DRP schemes assume α is real, thereby restricting the wave oscillations to be constant-amplitude. However, Brambley[14, 15] recently extended the consideration to non-constant-amplitude oscillations by allowing α to be complex, and demonstrated that DRP schemes are less efficient under these conditions compared to maximal order schemes. This issue is highlighted in figure 1 and figure 2. Given that non-constant-amplitude waves frequently occur in aeroacoustics, as evidenced by studies of acoustic linings where wave propagations can attenuate significantly [16], it is crucial to reassess the performance of these schemes in such practical applications.

Time-stepping schemes, like their spatial counterparts, can be analyzed in the wavenumber/frequency domain to optimize resolution performance. For instance, the solution to the time-stepping problem $\mathrm{d}\boldsymbol{U}/\mathrm{d}t = \boldsymbol{F}(\boldsymbol{U}, t)$ for the p-stage low-storage Runge–Kutta scheme considered by Hu, Hussaini, and Manthey [11] is given by

$$\boldsymbol{U}(t + \Delta t) = \boldsymbol{U}(t) + \beta_p \boldsymbol{K_p}, \qquad \text{where} \qquad \boldsymbol{K_{j+1}} = \Delta t \boldsymbol{F}\big(\boldsymbol{U}(t) + \beta_j \boldsymbol{K}_j,\, t + \beta_j \Delta t\big), \tag{4}$$

with $\beta_0 = 0$. Assuming $F(\boldsymbol{U}, t)$ is linear in $\boldsymbol{U}$ and time-invariant, and transforming the equation to the frequency domain (e.g., $F(\boldsymbol{U}, t) = -\mathrm{i}\omega\boldsymbol{U}$) yields

$$\boldsymbol{U}(t + \Delta t) = r(\omega\Delta t)\boldsymbol{U}(t), \qquad \text{where} \qquad r(\omega\Delta t) = 1 + \sum_{j=1}^{p} c_j(-\mathrm{i}\omega\Delta t)^j \qquad \text{and} \qquad \beta_{p-j} = c_{j+1}/c_j \tag{5}$$

with coefficient $c_1 = \beta_p$. For perfect time integrations, $\boldsymbol{U}(t + \Delta t)$ would equal $\boldsymbol{U}(t)r_e(\omega\Delta t)$, where $r_e(\omega\Delta t) = \exp\{-\mathrm{i}\omega\Delta t\}$. However, the numerical time integration by Runge–Kutta schemes present $\boldsymbol{U}(t+\Delta t) = \boldsymbol{U}(t)r(\omega\Delta t)$, where $r(\omega\Delta t) = \boldsymbol{U}(t)\exp\{-\mathrm{i}\bar{\omega}\Delta t\}$. Selecting coefficients $c_j = 1/j!$ minimizes the error $|r(\omega\Delta t) - r_e(\omega\Delta t)| = O\big((\Delta t)^{p+1}\big)$ in the limit $\Delta t \to 0$, defining this as a maximal order pth-order accurate scheme. Alternatively, adjusting the coefficients c_j can reduce the dispersion and dissipation errors of the Runge–Kutta schemes by minimizing an error of the form

$$E = \int_0^{\eta} |r(\omega\Delta t) - r_e(\omega\Delta t)|^2 \, \mathrm{d}(\omega\Delta t), \tag{6}$$

subject to constraints of a minimum order of accuracy (typically 2nd or 4th order accuracy as $\Delta t \to 0$) and stability (meaning $|r| \le 1$ for $0 \le \omega\Delta t < \eta_s$). Minimization of the error E have been performed by Hu et al. [11]. This minimization is the equivalent of the DRP developments for spatial derivative mentioned above for the spatial wavenumber $\alpha\Delta x$. Traditionally, optimizations of time-stepping schemes have assumed ω to be real. However, recent work by Petronilia and Brambley [18] considered non-constant-amplitude optimization, that is considering ω as complex. They suggested that the LDDRK56 schemes are sub-optimal and would be outperformed by higher order maximal order traditional Runge–Kutta schemes using longer timesteps at the equivalent computational costs. These findings are summarised in figure 3 and figure 4.

The objective of this paper is to evaluate the performance of current best practices in computational aeroacoustics (CAA), including the Dispersion-Relation-Preserving (DRP) scheme by Tam and Shen [3] and the LDDRK schemes

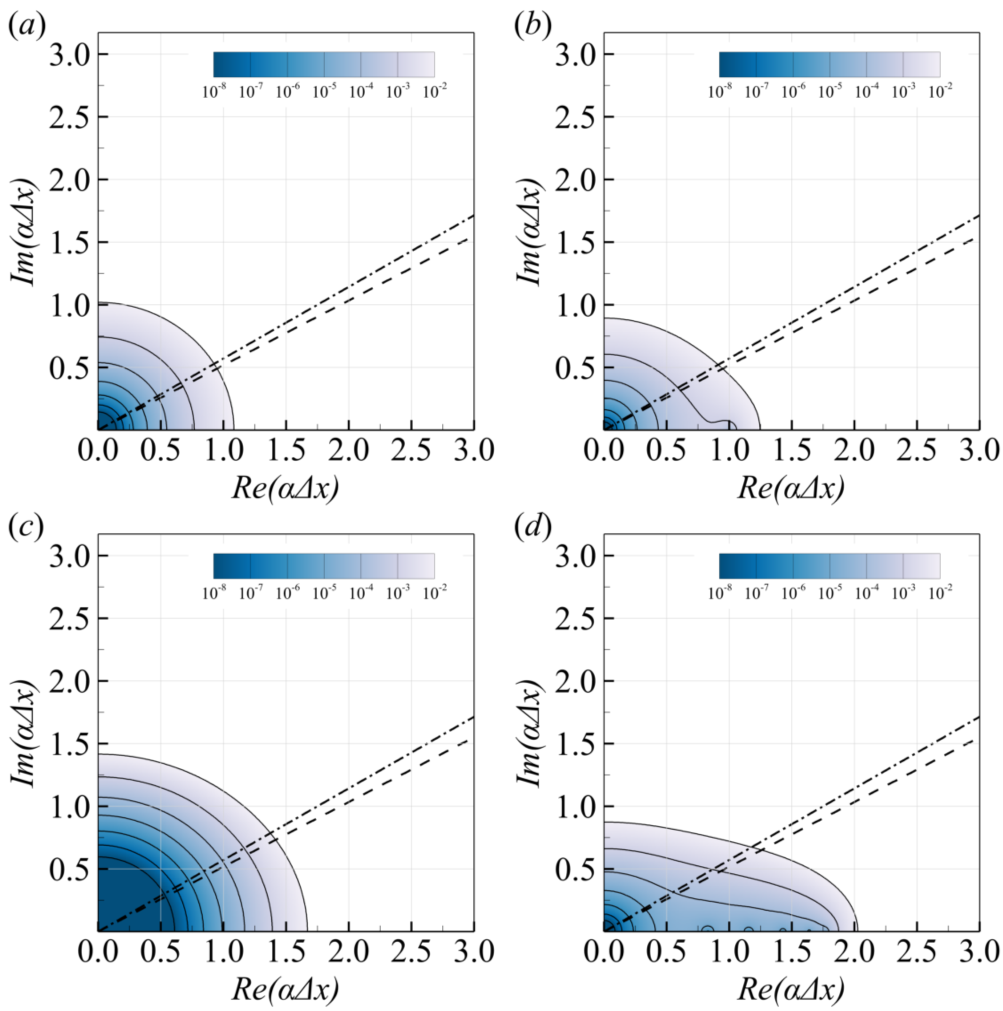

Fig. 1 Plots of $\varepsilon_p = |\bar{\alpha\Delta}x - \alpha\Delta x|$ in the complex α plane on a logarithmic scale to compare the absolute accuracy per unit mesh size of non-optimized and optimized explicit finite differences. The plots are divided as follows: (a) and (b) employ a 7-point scheme, while (c) and (d) utilize a 15-point scheme. Specifically, (a) MO7 and (c) MO15 are maximal-order schemes, and (b) DRP7 and (d) DRP15 are optimized 4th order schemes, developed according to Tam and Shen [3] and Tam [17], respectively. The dashed-dotted (-·-·) and dashed lines (- - -) represent variations in $\alpha\Delta x$ for different mesh sizes Δx, with and without flow conditions, for the axial wavenumbers analyzed by Tam et al. [16].

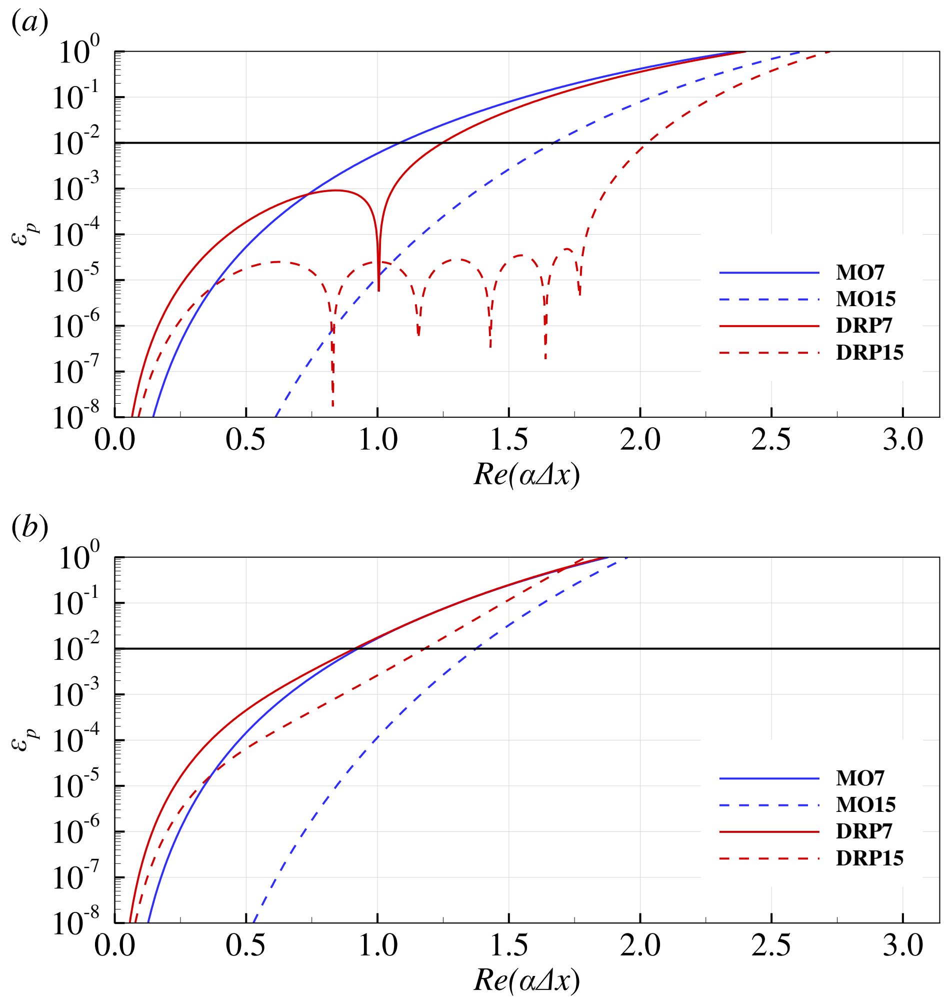

Fig. 2 Plots of $\varepsilon_p = |\alpha\bar{\Delta}x - \alpha\Delta x|$ along (*a*) the real axis (where Im$(\alpha\Delta x) = 0$) and (*b*) the dash-dotted line illustrated in figure 1. These plots compare non-optimized and optimized central finite difference schemes for constant and non-constant-amplitude waves propagation. A horizontal black line marks a 0.1% absolute error threshold per unit mesh size. Note that MO7 and MO15 represent maximal-order schemes, whereas DRP7 and DRP15 are optimized 4th order schemes, developed by Tam and Shen [3] and Tam [17], respectively.

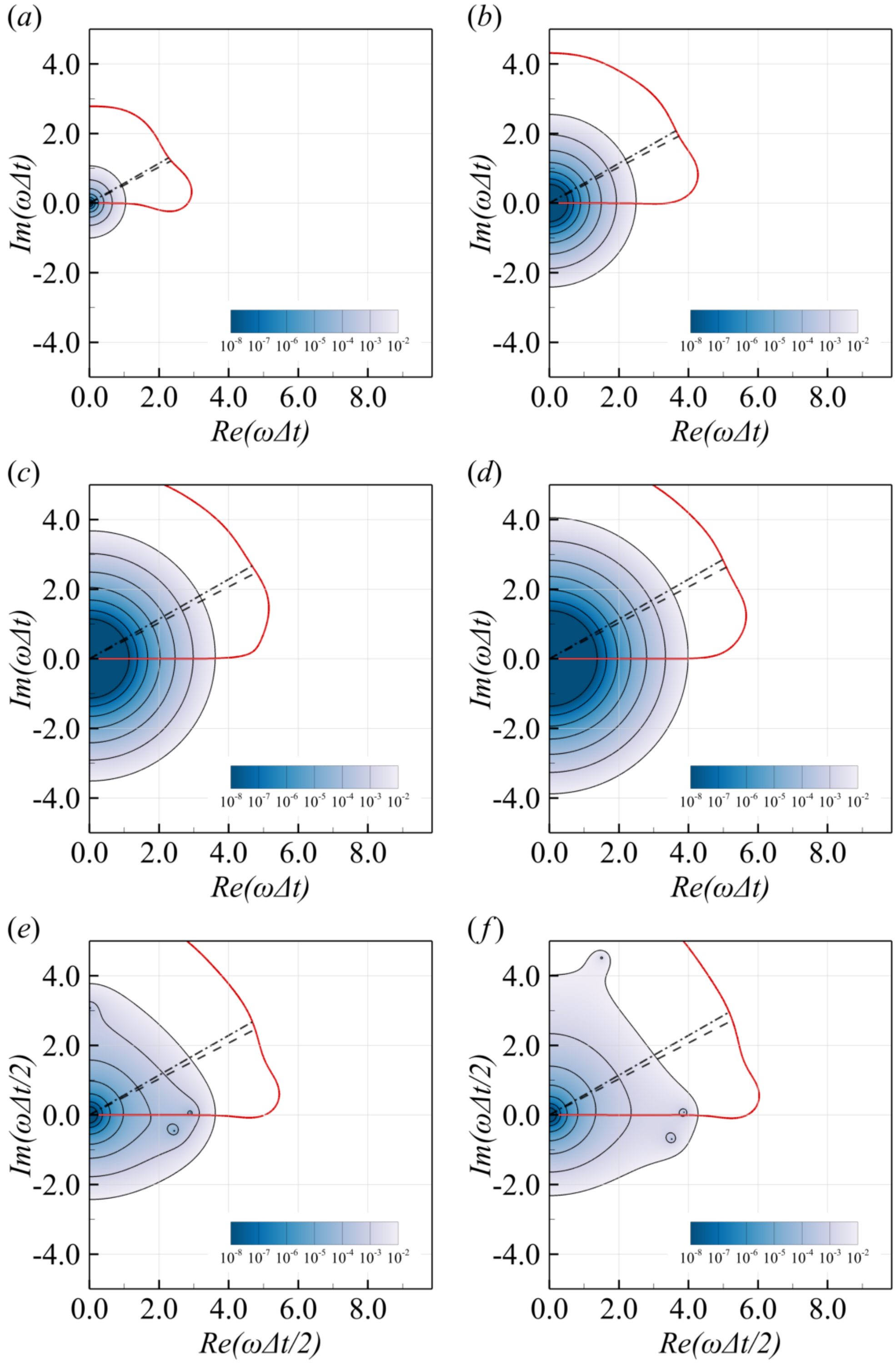

Fig. 3 Plots of $\varepsilon_p = |r(\omega\Delta t) - r_e(\omega\Delta t)|$ in the complex $\omega\Delta t$ plane for single-step maximal-order Runge-Kutta (RK) schemes with accuracy orders of (*a*) 4th, (*b*) 8th, (*c*) 11th, and (*d*) 12th, along with optimized two-step 4th-order LDDRK schemes (*e*) LDDRK46 and (*f*) LDDRK56, as described by Hu et al. [11]. The two-step LDDRK schemes utilize a halved time step of $\Delta t/2$ to ensure fair comparisons. The stability boundary for these schemes is delineated by a red solid line, indicating where $|r(\omega\Delta t)| = 1$.

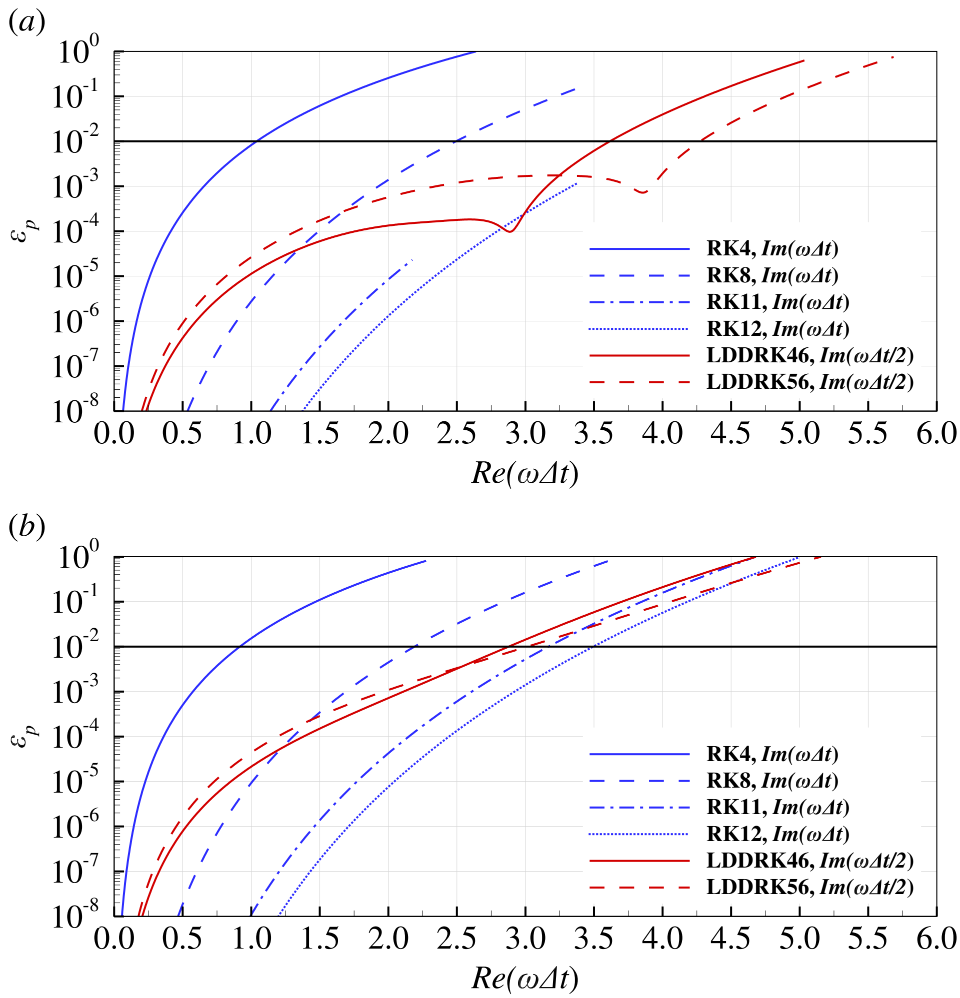

Fig. 4 Plots of $\varepsilon_p = |r(\omega\Delta t) - r_e(\omega\Delta t)|$ along the (*a*) real axis (i.e., Im$(\omega\Delta t) = 0$) and (*b*) dashed-dotted line shown in figure 3 for maximal-order RK and optimized LDDRK schemes of Hu et al. [11]. The horizontal black line indicates a threshold of 0.1% absolute error per unit time step. For clarity, the absolute error for RK schemes outside their stability region (i.e., where $|r(\omega\Delta t)| > 1$) are not included, to emphasize the comparison of their stability limits.

by Hu et al. [11]), against traditional non-optimized higher-order methods. Our analysis will focus on a standard CAA benchmark problem to determine whether these optimized schemes significantly improve accuracy and computational efficiency in practical scenarios, particularly in wave propagation problems featuring $O(1/r)$ decay of an expanding spherical acoustic wave.

II. Comparison with a realistic test case

In this section, the theoretical points above are illustrated through a 2D wave propagation example from Problem 1 of Category 3 of CAA benchmark test case of Hardin et al. [19]. Specifically, the linearized two-dimensional Euler equations on a uniform mean flow are considered

$$\frac{\partial \boldsymbol{Q}}{\partial t} + \frac{\partial \boldsymbol{E}}{\partial x} + \frac{\partial \boldsymbol{F}}{\partial y} = 0, \tag{7}$$

where

$$\boldsymbol{Q} = \begin{bmatrix} \rho' \\ u' \\ v' \\ p' \end{bmatrix}, \quad \boldsymbol{E} = \begin{bmatrix} M_x\rho' + u' \\ M_x u' + p' \\ M_x v' \\ M_x p' + u' \end{bmatrix}, \quad \boldsymbol{F} = \begin{bmatrix} M_y\rho' + v' \\ M_y u' \\ M_y v' + p' \\ M_y p' + v' \end{bmatrix}, \tag{8}$$

and $M_x = 0.5$, and $M_y = 0$ are constant mean flow Mach number in the x and y direction, respectively. The linearized equations have been non-dimensionless based on a spatial length scale d, the ambient speed of sound c_∞ for velocities, d/c_∞ for time scales and $\rho_\infty c_\infty^2$ for pressure, with density nondimensionalized by ρ_∞. The computational domain is embedded in free space and comprises of $x \in [-120, 120]$ in the streamwise direction and $y \in [-120, 120]$ in the vertical direction. The initial conditions prescribes a circular convective entropy wave and a circular acoustic wave as Gaussian impulses and are modelled as

$$\begin{aligned}
p' &= \epsilon_1 \exp\left[-\sigma_1\left(x^2 + y^2\right)\right], \\
\rho' &= \epsilon_1 \exp\left[-\sigma_1\left(x^2 + y^2\right)\right] + \epsilon_2 \exp\left[-\sigma_2\left((x-67)^2 + y^2\right)\right], \\
u' &= \epsilon_3 y \exp\left[-\sigma_3\left((x-67)^2 + y^2\right)\right], \\
v' &= -\epsilon_3 (x-67) \exp\left[-\sigma_3\left((x-67)^2 + y^2\right)\right],
\end{aligned}$$

where the physical parameters $\sigma_1 = \ln 2/9$, $\sigma_2 = \ln 2/25$, $\sigma_3 = \sigma_2$, $\epsilon_1 = 1.0$, $\epsilon_2 = 0.1$, $\epsilon_3 = 0.04$ are maintained according to original benchmark problem. All boundary conditions are imposed with the periodic boundary condition to enable direct application of symmetric finite differences. The domain is discretized using equally-spaced grid on x and y directions with $\Delta x = \Delta y = 2.0, 1.5$, and 1.0, respectively. The problem is solved using non-optimized centered finite difference schemes (i.e., 15-point maximal-order) and optimized (i.e., 7-point DRP and 15-point DRP), respectively. The single-step maximal-order RK4, RK8, RK12 and the two-step optimized LDDRK46 and LDDRK56 of Hu et al. [11] schemes are compared. The initial condition and the computed result of density and streamwise velocity fluctuations at solution time $t = 57$ are shown in figure 5 and figure 6, respectively. The absolute numerical error L_∞ is calculated using

$$L_\infty = \sup_{x \in [-120, 120]} |\boldsymbol{Q} - \boldsymbol{Q}_{exact}|, \tag{9}$$

where $\boldsymbol{Q}_{exact}$ are the analytical solution for the CAA benchmark problem. The computational effort is defined to be

$$\text{Effort} = pw(T/\Delta t)(L/\Delta x)(L/\Delta y), \tag{10}$$

where p is the number of Runge–Kutta stages, w is the half-width of the spatial derivative scheme (so the total width is $2w + 1$), $T = 57$ is the total simulation time, $L = 120$ is the simulation spatial length, and Δt, Δx, and Δy are the time step and mesh sizes. Comparison of the absolute error against the computational effort for non-optimized RK and optimized LDDRK schemes using the maximal-order 7-point, optimized DRP 7-point, maximal-order 15-point, and optimized DRP 15-point central finite difference schemes are shown in figure 7, 8, 9, and 10, respectively.

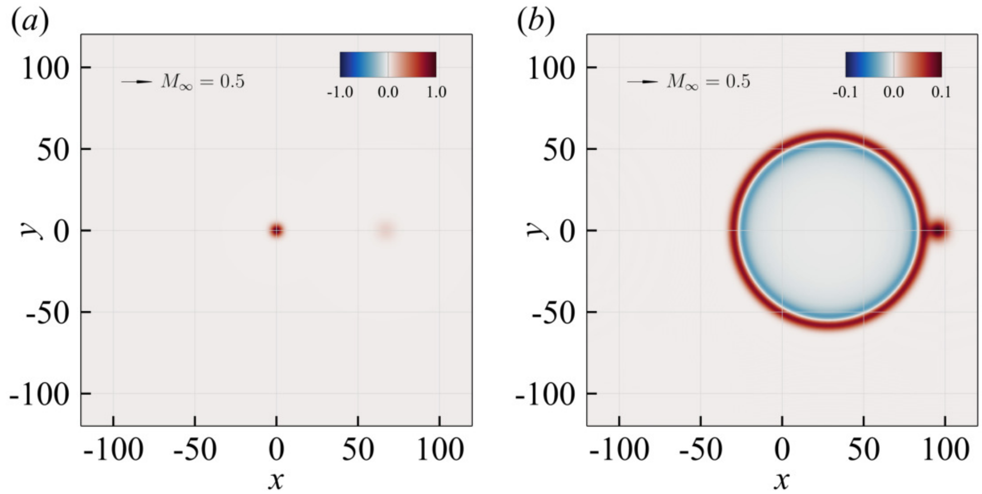

Fig. 5 Contour plots of density fluctuation ρ' of the acoustic and entropy waves at both (*a*) the initial condition at $t = 0$, and (*b*) the computed result at $t = 57$, respectively.

III. Conclusion

We solved a two-dimensional computational aeroacoustics (CAA) benchmark problem by applying both standard and optimized numerical schemes, then evaluating the respective numerical errors against the computational efforts. The findings reveal that optimized Dispersion-Relation Preserving (DRP) schemes do indeed outperform maximal-order central finite difference schemes in terms of spatial accuracy, as demonstrated by their lower error noise floors at larger mesh sizes (i.e., $\Delta x = \Delta y > 1.0$). However, for temporal accuracy, the optimized two-step Runge–Kutta schemes, such as LDDRK46 and LDDRK56, fail to provide significant benefits when aiming for an desired error threshold below 1% (i.e., $L_\infty < 0.01$), and indeed are outperformed by the RK8 and RK12 classical Runge–Kutta schemes when accuracy is limited by the time-integration rather than the spatial derivative (e.g. Figs. 9(c) and 10(c)); this is in agreement with the results of Petronilia and Brambley [18]. Conversely, when a more lenient error threshold above 1% is acceptable (i.e., $L_\infty > 0.01$), the classical RK4 method remains the preferred choice due to its greater stability limit per stage.

Acknowledgments

Y.W. Ho and E.J. Brambley gratefully acknowledges funding from the UK EPSRC (project EP/V002929/1).

References

[1] Sjögreen, B., and Yee, H. C., "Accuracy consideration by DRP schemes for DNS and LES of compressible flow computations," *Computers & fluids*, Vol. 159, 2017, pp. 123–136.

[2] Tam, C. K. W., and Webb, J. C., "Dispersion-Relation-Preserving Finite Difference Schemes for Computational Acoustics," *J. Comput. Phys.*, Vol. 107, 1993, pp. 262–281. https://doi.org/10.1006/jcph.1993.1142.

[3] Tam, C. K. W., and Shen, H., "Direct Computation of Nonlinear Acoustic Pulses using High-Order Finite Difference Schemes," AIAA paper 93-4325, 1993. https://doi.org/10.2514/6.1993-4325.

[4] Kim, J. W., and Lee, D. J., "Optimized Compact Finite Difference Schemes with Maximum Resolution," *AIAA J.*, Vol. 34, No. 5, 1996, pp. 887–893. https://doi.org/10.2514/3.13164.

[5] Kim, J. W., "Optimised Boundary Compact Finite Difference Schemes for Computational Aeroacoustics," *J. Comput. Phys.*, Vol. 225, 2007, pp. 995–1019. https://doi.org/10.1016/j.jcp.2007.01.008.

[6] Hixon, R., and Turkel, E., "Compact Implicit MacCormack-type Schemes with High Accuracy," *J. Comput. Phys.*, Vol. 158, No. 1, 2000, pp. 51–70. https://doi.org/10.1006/jcph.1999.6406.

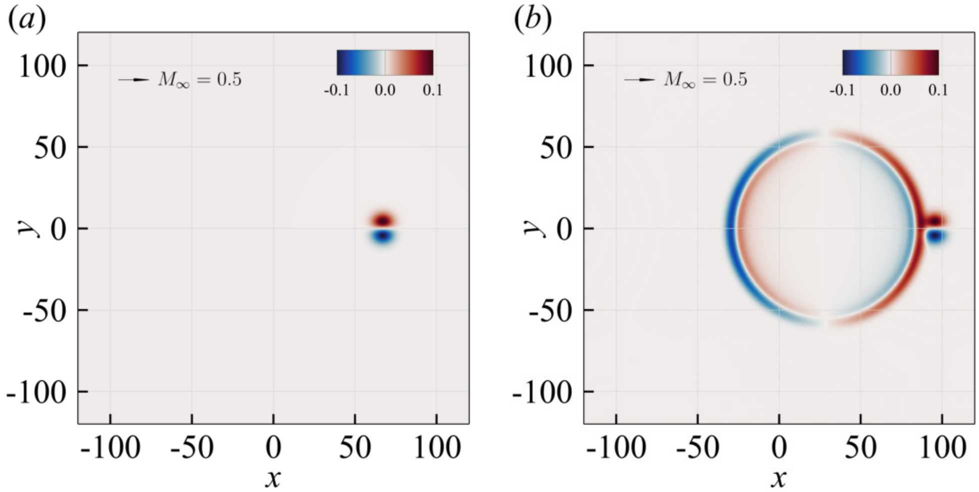

Fig. 6 Contour plots of streamwise velocity fluctuation u', associated with the vorticity wave at the (*a*) initial condition at $t = 0$, and (*b*) computed result at $t = 57$, respectively.

[7] Tang, L., and Baeder, J. D., "Uniformly Accurate Finite Difference Schemes for p-Refinement," *SIAM J. Sci. Comput.*, Vol. 20, No. 3, 1999, pp. 1115–1131. https://doi.org/10.1137/S1064827596308354.

[8] Bogey, C., and Bailly, C., "A Family of Low Dispersive and Low Dissipative Explicit Schemes for Flow and Noise Computations," *J. Comput. Phys.*, Vol. 194, 2004, pp. 194–214. https://doi.org/10.1016/j.jcp.2003.09.003.

[9] Berland, J., Bogey, C., Marsden, O., and Bailly, C., "High-order, Low Dispersive and Low Dissipative Explicit Schemes for Multiple-scale and Boundary Problems," *J. Comput. Phys.*, Vol. 224, 2007, pp. 637–662. https://doi.org/10.1016/j.jcp.2006.10.017.

[10] Turner, J. M., Haeri, S., and Kim, J. W., "Improving the Boundary Efficiency of a Compact Finite Difference Scheme through Optimising its Composite Template," *Computers & Fluids*, Vol. 138, 2016, pp. 9–25. https://doi.org/10.1016/j.compfluid.2016.08.007.

[11] Hu, F. Q., Hussaini, M. Y., and Manthey, J. L., "Low-Dissipation and Low-Dispersion Runge–Kutta Schemes for Computational Acoustics," *J. Comput. Phys.*, Vol. 124, 1996, pp. 177–191. https://doi.org/10.1006/jcph.1996.0052.

[12] Rona, A., Spisso, I., Hall, E., Bernardini, M., and Pirozzoli, S., "Optimised Prefactored Compact Schemes for Linear Wave Propagation Phenomena," *J. Comput. Phys.*, Vol. 328, 2017, pp. 66–85. https://doi.org/10.1016/j.jcp.2016.10.014.

[13] Brambley, E. J., "Asymmetric Finite Differences for Non-Constant-Amplitude Waves," *Proc. International Congress on Sound and Vibration, London, 23–27 July*, 2017. URL http://www.warwick.ac.uk/staff/E.J.Brambley/files/brambley-2017-icsv.pdf.

[14] Brambley, E. J., "DRP schemes perform poorly for decaying or growing oscillations," AIAA paper 2015-2540, 2015. https://doi.org/10.2514/6.2015-2540.

[15] Brambley, E. J., "Optimized finite-difference (DRP) schemes perform poorly for decaying or growing oscillations," *J. Comput. Phys.*, Vol. 324, 2016, pp. 258–274. https://doi.org/10.1016/j.jcp.2016.08.003.

[16] Tam, C. K. W., Ju, H., and Chien, E. W., "Scattering of Acoustic Duct Modes by Axial Liner Splices," *J. Sound Vib.*, Vol. 310, 2008, pp. 1014–1035. https://doi.org/10.1016/j.jsv.2007.08.027.

[17] Tam, C. K. W., *Computational Aeroacoustics*, Cambridge, 2012, Chap. 2.

[18] Petronilia, A., and Brambley, E. J., "Optimized Runge–Kutta (LDDRK) schemes with non-constant-amplitude waves," AIAA paper 2019-2414, 2019. https://doi.org/10.2514/6.2019-2414.

[19] Hardin, J. C., Ristorcelli, J. R., and Tam, C. K. W., "ICASE/LaRC Workshop on Benchmark Problems in Computational Aeroacoustics (CAA)," 1995.

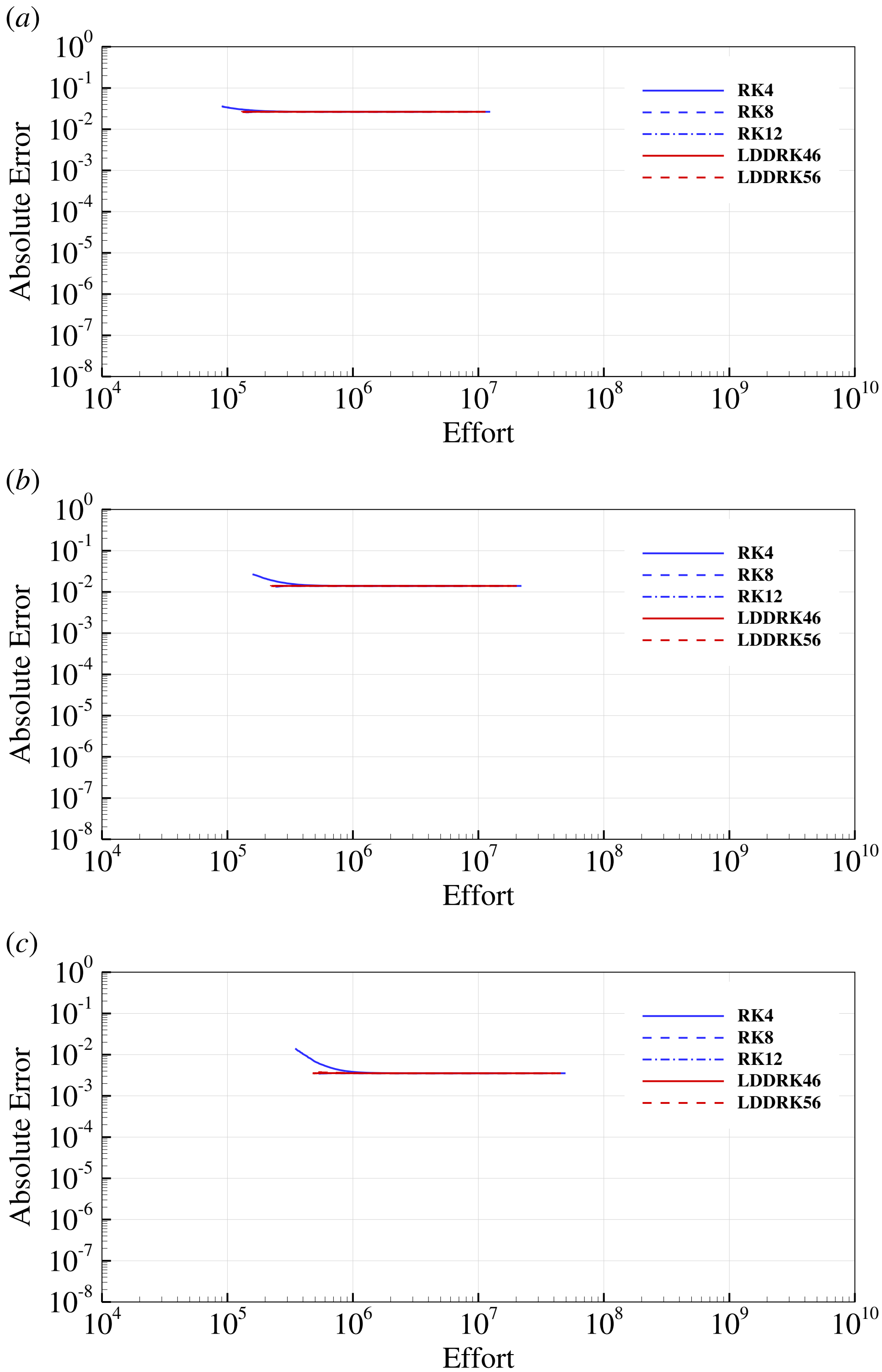

Fig. 7 Comparison of the absolute error against the computational effort required for unoptimized and optimized RK schemes using the maximal-order 7-point central finite difference for (*a*) $\Delta x = \Delta y = 2.0$, (*b*) 1.5, and (*c*) 1.0.

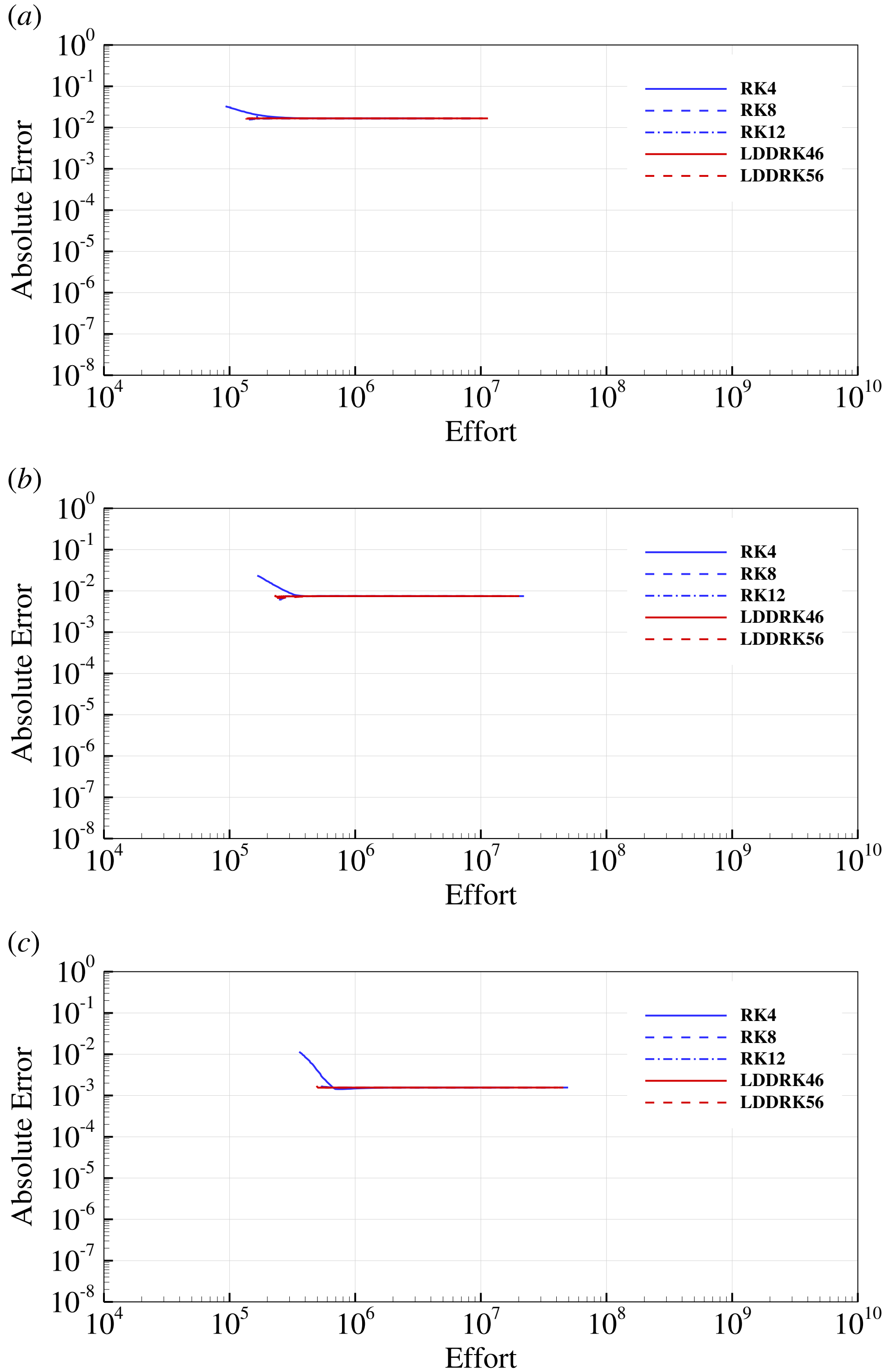

Fig. 8 Comparison of the absolute error against the computational effort required for unoptimized and optimized RK schemes using the optimized DRP 7-point central finite difference for (*a*) $\Delta x = \Delta y = 2.0$, (*b*) 1.5, and (*c*) 1.0.

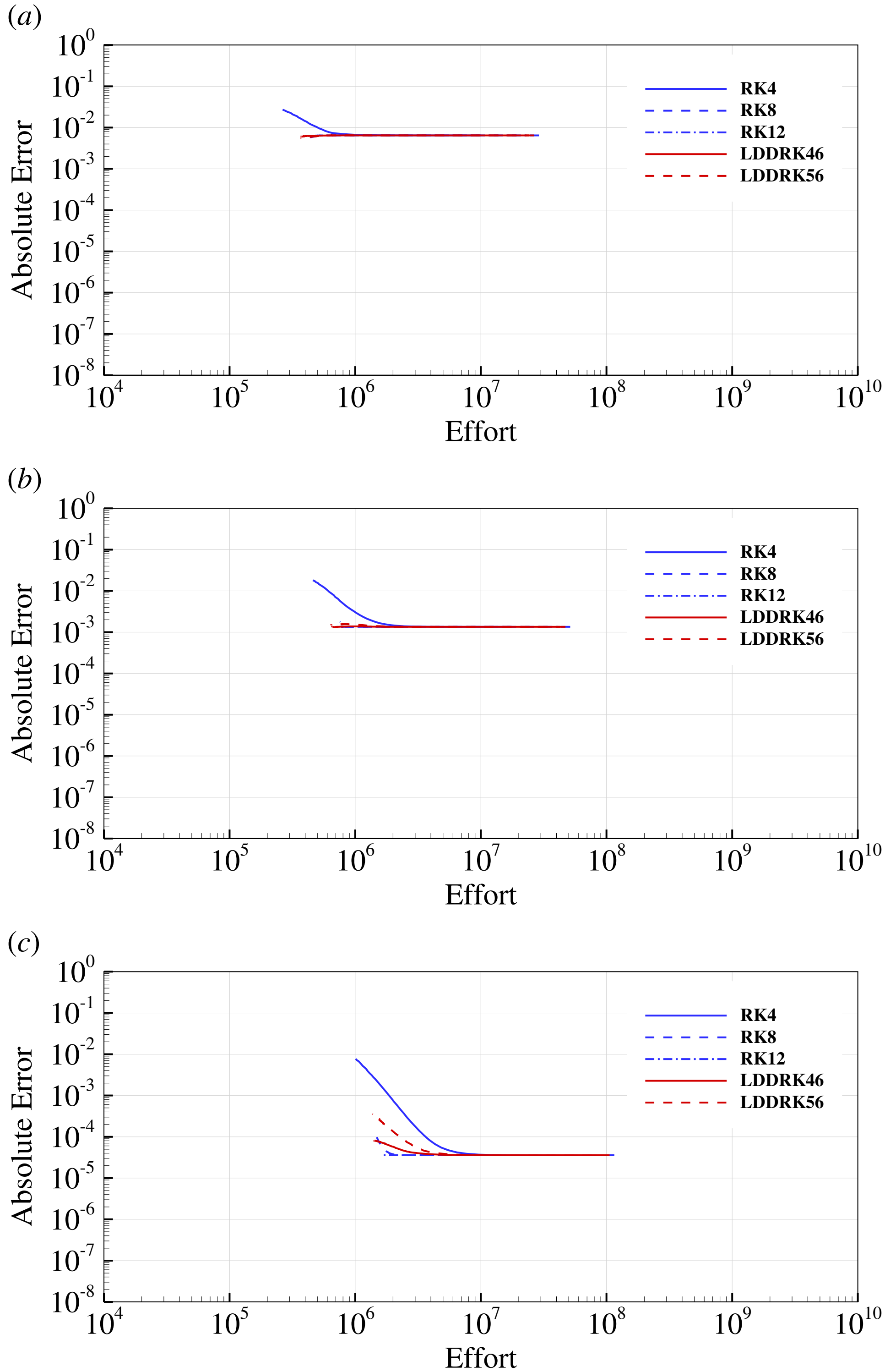

Fig. 9 Comparison of the absolute error against the computational effort required for unoptimized and optimized RK schemes using the maximal-order 15-point central finite difference for (*a*) $\Delta x = \Delta y = 2.0$, (*b*) 1.5, and (*c*) 1.0.

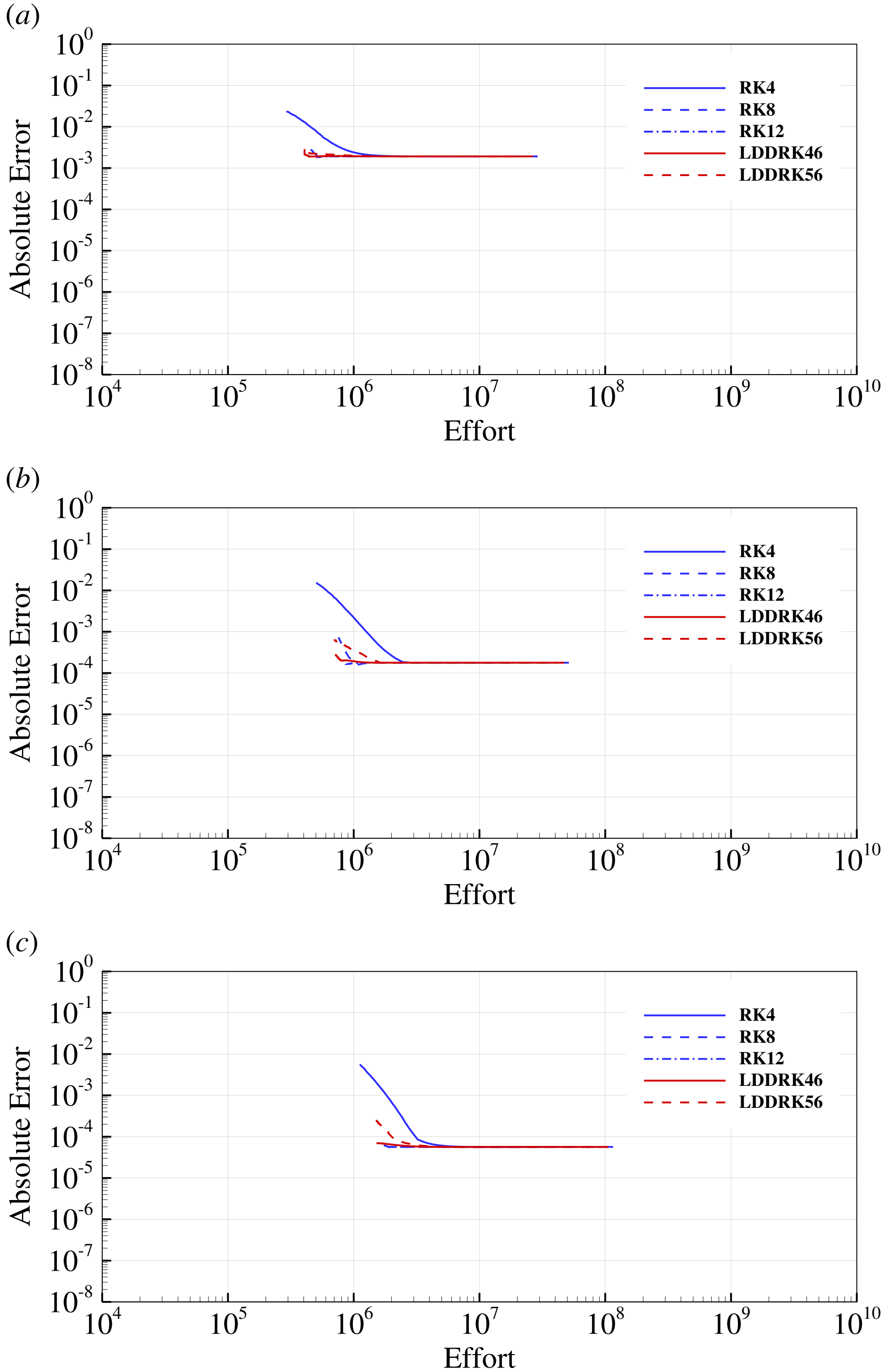

Fig. 10 Comparison of the absolute error against the computational effort required for unoptimized and optimized RK schemes using the optimized DRP 15-point central finite difference for (*a*) $\Delta x = \Delta y = 2.0$**, (*b*)** 1.5**, and (*c*)** 1.0**.**